Gfi1b controls integrin signaling-dependent cytoskeleton dynamics and organization in megakaryocytes

Hugues Beauchemin,[1] Peiman Shooshtarizadeh,[1] Charles Vadnais,[1] Lothar Vassen,[1] Yves D Pastore[2] and Tarik Möröy[1,3,4]

[1]Institut de Recherches Cliniques de Montréal, IRCM, QC; [2]Département de Pédiatrie, Service d'Hématologie et Oncologie, CHU Ste-Justine, Montréal, QC; [3]Département de Microbiologie, Infectiologie et Immunologie, Université de Montréal, QC and [4]Division of Experimental Medicine, McGill University, Montréal, QC, Canada

Haematologica 2017
Volume 102(3):484-497

ABSTRACT

Mutations in *GFI1B* are associated with inherited bleeding disorders called *GFI1B*-related thrombocytopenias. We show here that mice with a megakaryocyte-specific *Gfi1b* deletion exhibit a macrothrombocytopenic phenotype along a megakaryocytic dysplasia reminiscent of *GFI1B*-related thrombocytopenia. GFI1B deficiency increases megakaryocyte proliferation and affects their ploidy, but also abrogates their responsiveness towards integrin signaling and their ability to spread and reorganize their cytoskeleton. *Gfi1b*-null megakaryocytes are also unable to form proplatelets, a process independent of integrin signaling. GFI1B-deficient megakaryocytes exhibit aberrant expression of several components of both the actin and microtubule cytoskeleton, with a dramatic reduction of α-tubulin. Inhibition of FAK or ROCK, both important for actin cytoskeleton organization and integrin signaling, only partially restored their response to integrin ligands, but the inhibition of PAK, a regulator of the actin cytoskeleton, completely rescued the responsiveness of *Gfi1b*-null megakaryocytes to ligands, but not their ability to form proplatelets. We conclude that *Gfi1b* controls major functions of megakaryocytes such as integrin-dependent cytoskeleton organization, spreading and migration through the regulation of PAK activity whereas the proplatelet formation defect in GFI1B-deficient megakaryocytes is due, at least partially, to an insufficient α-tubulin content.

Correspondence:
tarik.moroy@ircm.qc.ca

Received: May 31, 2016.
Accepted: January 11, 2017.
Pre-published: January 12, 2017.

doi:10.3324/haematol.2016.150375

Check the online version for the most updated information on this article, online supplements, and information on authorship & disclosures: www.haematologica.org/content/102/3/484

Introduction

Platelets are small circulating cell fragments essential for blood clotting. The normal platelet count in humans is 150-400x10^9/L. The short life span of platelets is compensated by the continuous process of thrombopoiesis (ongoing platelet production) by highly specialized polyploid cells called megakaryocytes that form protrusions named "proplatelets" from which platelets are released into the bloodstream.[1] Thrombocytopenia is a disorder defined by low platelet counts caused by different conditions ranging from autoimmune destruction of platelets to the complete absence of platelet-producing megakaryocytes.[2,3] Three recent studies in patients exhibiting macrothrombocytopenia associated with megakaryocytic dysplasia have identified the transcription factor GFI1B as being responsible for a novel platelet syndrome[4-6] named "*GFI1B*-related thrombocytopenia" (*GFI1B*-RT)[7] or "Bleeding Disorder, Platelet-Type, 17" (BDPLT17) as listed in the OMIM database (http://www.omim.org/entry/187900).

Previous reports of a potential role for *Gfi1b* in thrombopoiesis showed that GFI1B deficiency led to a severe impairment of both erythropoiesis and thrombopoiesis in mice[8,9] and that acute ablation of *Gfi1b* in adult animals is lethal due to erythropoietic failure, confirming the role of *Gfi1b* in late erythropoiesis.[10-12] To circumvent this limitation and to analyze how *Gfi1b* regulates both megakarypoiesis and thrombopoiesis, we crossed mice carrying conditional *Gfi1b* alleles (*Gfi1b*$^{fl/fl}$)[13]

either with animals expressing a megakaryocyte-specific Pf4-Cre transgene[14] or with *Rosa*-Cre-ERT transgenic mice that enable a tamoxifen-inducible deletion.[11] We showed before that by inducing Cre activity in *Rosa*-Cre-ERT *Gfi1b*$^{fl/fl}$ mice using a suboptimal dose of tamoxifen, the block in erythroid maturation can be prevented by allowing the formation of erythroblasts that retain non-deleted *Gfi1b* alleles.[11]

Here we show that this strategy allows the mice to survive and induces a strong expansion of megakaryocytes with fully excised *Gfi1b* alleles. This permitted the analysis of GFI1B-deficient megakaryocytes, and allowed us to demonstrate precisely how *Gfi1b* acts in both early and late stages of megakaryocytic differentiation. At early stages of megakaryocyte maturation, *Gfi1b* controls megakaryocyte polyploidization and motility. At later stages, the loss of GFI1B disrupts cytoskeleton organization and blocks platelet formation. Here, we present evidence that *Gfi1b* exerts its function in cellular spreading and motility by controlling integrin signaling pathways principally through the inhibition of p21-activated kinases (PAKs), whereas the defect of proplatelet formation can be explained by a microtubule defect due to an almost complete absence of α-tubulin in GFI1B-deficient cells.

Methods

Mice

The protocol for this research was reviewed and assessed by the Animal Care Committee (ACC, #2013-04) of the Clinical Research Institute in Montréal and all the animals used in this experiment were cared for in compliance with the Canadian Council on Animal Care (www.ccac.ca) guidelines and principles.

In vitro culture of megakaryocytes

Bone marrow cells were lineage (B220$^-$Mac-1$^-$Gr-1$^-$CD16/32$^-$) depleted on an AutoMACS Pro system (Miltenyi) and suspended in StemSpan SFEM (StemCell Technologies) supplemented with 2.6% fetal bovine serum, 1% L-glutamine and stem cell factor (20 ng/mL) then cultured for 2 days at 37°C in 5% CO_2. Cells were transferred into fresh medium containing thrombopoietin (50 ng/mL) and cultured for 4 more days. Mature megakaryocytes were enriched on a bovine serum albumin gradient as previously described[15] and plated in 12-well μ-Chamber glass slides (ibidi) coated with fibronectin (500 μg/mL; Life Technology), fibrinogen (100 μg/mL; Hyphen BioMed) or collagen (1:20; StemCell Technologies). Cells were then allowed to spread for 3-8 h. Cells were fixed in μ-Chamber slides with 4% formaldehyde/phosphate-buffered saline, permeabilized with 0.1% Triton-X100/phosphate-buffered saline and blocked with FcBlock (1:500; BD Biosciences), then labeled with FITC-CD41 (BD Biosciences) and AF555-β-tubulin (Cell Signaling) antibodies or AF555-Phalloidin (Molecular Probes). All conditions for both controls and knockouts were applied to the same μ-Chamber slide to minimize variation between samples.

Results

Severe thrombocytopenia associated with the loss of *Gfi1b* expression

We generated a megakaryocyte-specific knockout of *Gfi1b* using *Pf4*-Cre and *Rosa*-Cre-ERT mice (Figure 1). *Pf4*-Cre deletes only in mature *Gfi1b*$^{wt/fl}$ megakaryocytes (>70%) but in *Gfi1b*$^{fl/fl}$ megakaryocyte deletion starts earlier and with higher efficiency (>99%) (Figure 1D) probably due to a de-repression of the *Pf4* promoter in the absence of GFI1B. *Pf4*-Cre *Gfi1b*$^{fl/fl}$ mice were viable, but showed internal bleeding and a 1,000-fold reduction of platelets owing to a failure of platelet production rather than a clearance of circulating platelets (Figure 2A-C). Since the *Pf4*-Cre transgene is active only from late megakaryocyte progenitors to mature megakaryocytes (Figure 1D), we also used the *Rosa*-Cre-ERT transgene, enabling a tamoxifen-inducible acute ablation of Gfi1b in adult mice. The two-color *Rosa*$^{mT/mG}$ reporter strain shows efficient ablation from lin$^-$cKit$^+$Sca1$^+$ (LSK) cells to mature megakaryocytes (Figure 1D). By reducing tamoxifen doses, we were able to obtain a good excision rate of the floxed *Gfi1b* alleles in megakaryocytes, while allowing erythroid cells to escape arrest and the mice to survive (Figure 1B-E). In this model, tamoxifen provoked a reduction of circulating platelets by day 4 after the first injection, which was followed by rapid clearance leading to a minimal platelet level 3 days later (Figure 2D, E). A reduction of reticulated platelets was observed as early as 2-3 days after the first tamoxifen injection (Figure 2D-F), suggesting that platelet production stops shortly after *Gfi1b* ablation. A thrombocytopenic state is maintained in GFI1B-deficient mice even several months after tamoxifen injections, excluding the possibility of a transient effect (Figure 2E).

MGG-stained blood smears confirmed the reduction of circulating platelets in the *Rosa*-Cre-ERT *Gfi1b*$^{fl/fl}$ mice and an almost complete absence of platelets in the *Pf4*-Cre *Gfi1b*$^{fl/fl}$ mice. Some rare remaining platelets detected in both models showed a larger perimeter and lower α-granule content (Figure 2G), reminiscent of the platelets seen in *GFI1B*-RT. A cytospin from plasma confirmed this and showed large and highly vacuolar platelets which resembled megakaryocytic fragments (Figure 2H) similar to those seen in GPIbα knockout mice.[16] Platelets from both mice were also globally larger than those from controls (Figure 2I).

Loss of GFI1B drives megakaryocyte expansion

In *Pf4*-Cre *Gfi1b*$^{fl/fl}$ mice, the number of megakaryocytes defined as lin$^-$CD41$^+$CD61$^+$ was increased 3- to 4-fold compared to controls (Figure 3A). This was accompanied by an equivalent increase of megakaryocyte precursors able to form colonies (CFU-Mk), which were otherwise indistinguishable from controls with regards to cell number or morphology (Figure 3B). Megakaryocyte expansion was even more pronounced in *Rosa*-Cre-ERT *Gfi1b*$^{fl/fl}$ mice, in which an already detectable increased cellularity 3 days after tamoxifen injection gradually reached a >25-fold increase after 2 months (Figure 3C,D and *Online Supplementary Figure S1A*). This megakaryocyte expansion was independent of the thrombocytopenic state since it started 1 day before the loss of platelets became apparent and thrombopoietin levels were not affected in the knockout animals (*data not shown*). Colony-forming assays from *Rosa*-Cre-ERT *Gfi1b*$^{fl/fl}$ mice showed a proportional increase in CFU-Mk numbers (Figure 3E and *Online Supplementary Figure S1B*). In contrast to cells from *Pf4*-Cre *Gfi1b*$^{fl/fl}$ mice, cells from *Rosa*-Cre-ERT *Gfi1b*$^{fl/fl}$ mice gave rise to colonies with fewer and smaller cells than control CFU-Mk and reminiscent of an immature state (Figure 3E and *Online Supplementary Figure S1C*). A colony assay was

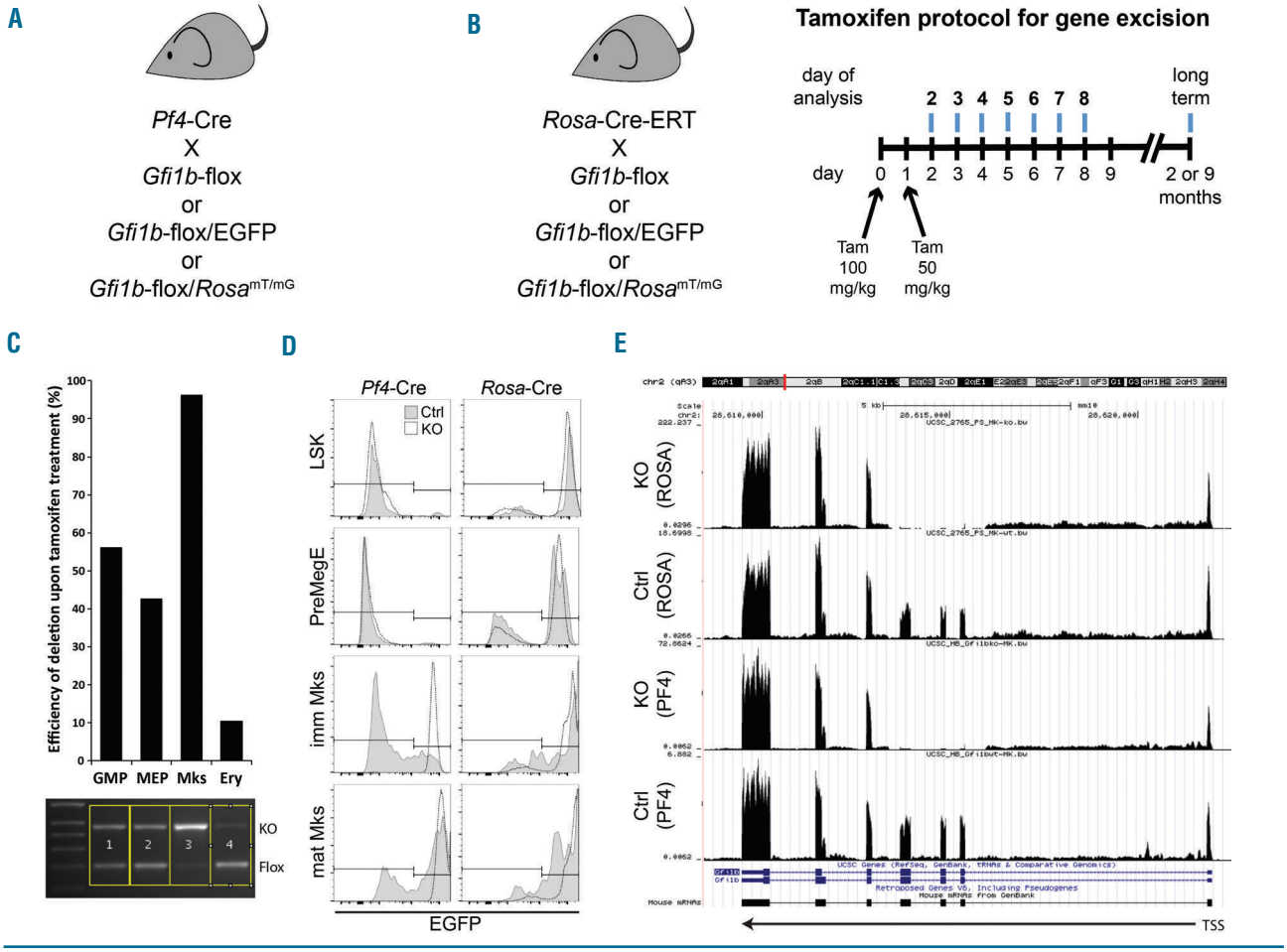

Figure 1. Strategies and efficiencies of *Gfi1b* deletion in two mouse models. (A) The *Pf4-Cre* transgene that drives Cre expression only in megakaryocytes was introduced by breeding into either *Gfi1b*$^{fl/fl}$ (carrying two floxed alleles) and *Gfi1b*$^{wt/fl}$ (carrying one floxed allele and one wild-type allele) mice, the *Gfi1b*$^{fl/EGFP}$ (carrying one floxed allele and one EGFP-knock-in allele) and *Gfi1b*$^{wt/EGFP}$ (carrying one wild-type allele and one EGFP-knock-in allele) that allowed for visualization of megakaryocytes and progenitor cells, or *Gfi1b*$^{fl/fl}$ and *Gfi1b*$^{wt/fl}$ mice also carrying the *Rosa*$^{mT/mG}$ reporter gene to monitor Cre activity. (B) The *Rosa*-Cre-ERT locus that drives Cre-ERT expression in all cell types upon tamoxifen treatment was introduced into *Gfi1b*$^{fl/fl}$ and *Gfi1b*$^{wt/fl}$, *Gfi1b*$^{fl/EGFP}$ and *Gfi1b*$^{wt/EGFP}$, and *Gfi1b*$^{fl/fl}$ and *Gfi1b*$^{wt/fl}$ *Rosa*$^{mT/mG}$ mice as in (A). Suboptimal doses of tamoxifen were injected at 100 mg/kg on day 0 followed by 50 mg/kg the day after and mice analyzed either from day 2-8 for short-term experiments or after 2 or 9 months for long-term experiments. (C) Efficiency of tamoxifen-induced *Gfi1b*-depletion in the mice from (B) 2 months after injection was assessed by polymerase chain reaction amplification of the *Gfi1b*-locus in some hematopoietic cellular subsets to see the conversion of the floxed (Flox) allele toward the knockout (KO) allele. GMP: granulocyte-macrophage progenitor; MEP: megakaryocyte-erythroid progenitor; Mks: megakaryocytes; Ery: erythroid cells. (D) The specificity of the two Cre models shown in (A) and (B) was also assessed using *Rosa*$^{mT/mG}$ reporter mice in which cells become EGFP positive upon Cre activation. In *Pf4*-Cre mice, the Cre was active mainly in the later stages of megakaryocyte maturation, although a little earlier in the knockout but was not present in PreMegE or LSK. In the *Rosa*-Cre-ERT, the Cre was active in all hematopoietic lineages but more prominent in maturing megakaryocytes. (E) Visualization of the alignment tracks obtained through the UCSC genome browser of the *Gfi1b* locus taken from the RNA-Seq analyses (Figure 7) of *Rosa*-Cre-ERT *Gfi1b*$^{fl/fl}$ [KO (ROSA)] and *Gfi1b*$^{wt/fl}$ [Ctrl (ROSA)] or *Pf4*-Cre *Gfi1b*$^{fl/fl}$ [KO (PF4)] *Gfi1b*$^{wt/fl}$ [Ctrl (PF4)] showing the absence of exons 2-4 in the knockout, confirming its efficiency, the first exon being on the right. TSS: transcription start site.

done with sorted lin$^-$Kit$^+$ (LK) cells from *Rosa*-Cre-ERT *Gfi1b*$^{fl/fl}$ also carrying the *Rosa*$^{mT/mG}$ two-color Cre reporter allele expressing red fluorescence prior to Cre exposure and green fluorescence in Cre-expressing cells having actively excised floxed genomic regions. GFP$^+$ (*Gfi1b* deleted) LK produced CFU-Mk containing small acetylcholinesterase-positive cells whereas Tomato$^+$ (*Gfi1b* not deleted) LK from the same mice produced phenotypically normal CFU-Mk (Figure 3F), demonstrating that the aberrant megakaryocyte phenotype is intrinsic to *Gfi1b*-deleted cells.

Abnormal morphology and endomitosis in *Gfi1b*-null megakaryocytes

Compared to controls, GFI1B-deficient megakaryocytes had a hyperlobulated nucleus with an abnormal cellular localization, forming a ring around the cell's inner membrane instead of occupying a more central localization as seen in controls and were reminiscent of the staghorn-shaped nucleus of megakaryocytes observed in patients with essential thrombocythemia.[17] The ultrastructure of GFI1B-deficient megakaryocytes was also poorly defined with an absence of distinct marginal and intermediate zones despite the presence of a few granules that tended to remain gathered (Figure 4A,B).

A culture in suspension of megakaryocytes from *Rosa*-Cre-ERT *Gfi1b*$^{EGFP/fl}$ mice, which express GFP under the control of the Gfi1b promoter mainly in megakaryocytes and precursors, contained high numbers of smaller green cells that were not present in the control (Figure 4C). To investigate whether these smaller cells were megakaryocytes or megakaryocyte precursors, we stained mature megakaryocytes (lin$^-$CD9^{high}CD41^{high}cKit$^+$CD61^{high}) from both *Pf4*-Cre and *Rosa*-Cre-ERT *Gfi1b*$^{fl/fl}$ mice with

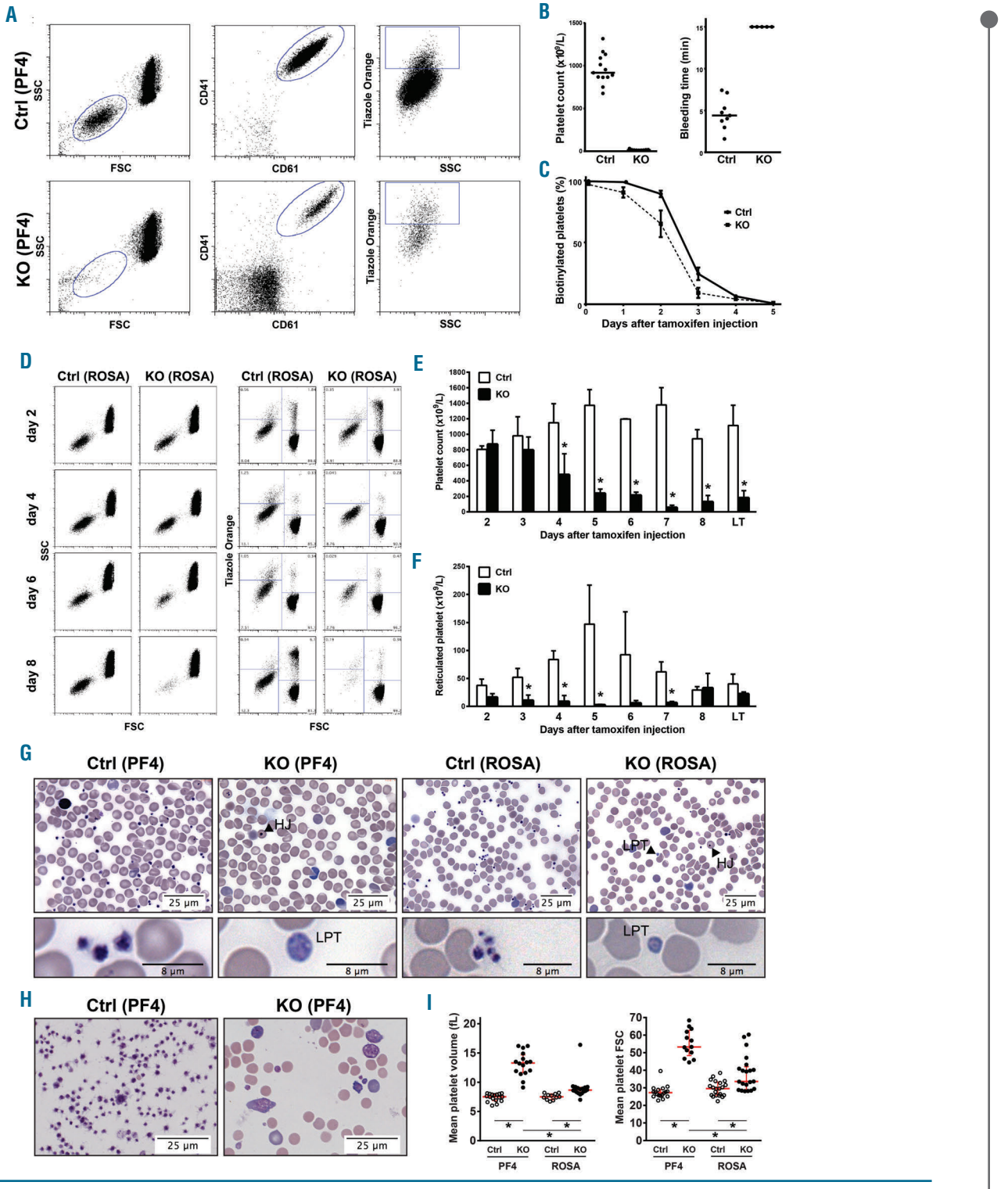

Figure 2. The loss of GFI1B causes a severe thrombocytopenia. (A) FACS analysis of circulating platelets from *Pf4*-cre *Gfi1b*$^{wt/fl}$ control [Ctrl (PF4)] and *Pf4*-cre *Gfi1b*$^{fl/fl}$ knockout mice [KO (PF4)]. Platelets are first identified based on their FSC/SSC profile, then true platelets are identified as being CD41^{+} CD61^{+}. Thiazole orange staining identifies reticulated platelets. (B) Quantitation of circulating platelets in the *Pf4*-cre *Gfi1b*$^{fl/fl}$ knockout mice (n = 9) compared to the controls (n = 13; Student *t*-test: *P*=0) and bleeding time [WT (n = 9) and KO (n = 5); Mann-Whitney *U*-test: *P*<0.0001]. All knockout animals reached the maximum bleeding time allowed without demonstrating signs of blood clotting. (C) Platelet lifespan was assessed *in vivo* in *Pf4*-cre *Gfi1b*$^{fl/fl}$ (n = 5) and *Pf4*-cre *Gfi1b*$^{wt/fl}$ (n = 4) mice after biotin labeling of platelets through intravenous injection of Sulfo-NHS-biotin. Blood was analyzed as in (A) during 5 days after biotin labeling and the percentage of biotinylated platelets assessed by FACS. (D-F) Kinetics of platelet disappearance upon tamoxifen injection in *Rosa*-Cre-ERT *Gfi1b*$^{fl/fl}$ and *Rosa*-Cre-ERT *Gfi1b*$^{wt/fl}$ animals (n = 3 per time point). Animals received 100 mg/kg tamoxifen on day 0 and 50 mg/kg on day 1. Blood samples were analyzed on an Advia Hematology System and by flow cytometry (D). (E) The number of platelets given as mean count per liter ± SD. (F) The number of reticulated platelets given as mean count per liter ± SD. LT: a long-term analysis done 2 months after tamoxifen injection. Student *t*-test: (*) marks statistical significance (*P*<0.05). (G) Representative MGG-stained blood smears of *Pf4*-cre *Gfi1b* controls and knockouts [Ctrl (PF4) and KO (PF4)] and *Rosa*-Cre-ERT *Gfi1b* controls and knockouts [Ctrl (ROSA) and KO (ROSA)] showing in the knockouts a reduced number of platelets, the presence of large platelets with a lower granularity (LPT) and erythrocytes exhibiting Howell-Jolly bodies (HJ). (H) MGG-stained platelet cytospin showing the presence of very large vacuolar platelets specifically in the knockouts. (I) Comparison of the mean platelet volume measured on an Advia 120 cell analyzer (left) and the mean platelet forward scatter measured by FACS on CD41^{+}CD61^{+} cells (FSC; right) in the *Pf4*-Cre *Gfi1b*$^{fl/fl}$ (PF4) and the *Rosa*-Cre *Gfi1b*$^{fl/fl}$ (ROSA) mice and their respective controls. the red lines represent the median ± interquartile rage. Kruskal-Wallis test: *P*<0.0001. * indicates statistical differences as determined using the *post hoc* Dunn multiple comparison test.

Hoechst to assess their ploidy (*Online Supplementary Figure S2A*). In control mice, most of these cells were polyploid (>4N) with a 16N population being predominant (~60% of all megakaryocytes) followed by the 8N and 32N populations, each representing 10-20%, and a very low number of 64N cells (Figures 4D and *Online Supplementary Figure S2A*), which is in agreement with previous reports.[18,19] Megakaryocytes from *Pf4*-Cre Gfi1b$^{fl/fl}$ mice were also polyploid, but had a different distribution: the 32N subset was not affected by Gfi1b loss, the 16N megakaryocytes were notably decreased and the 2N, 4N and 8N fractions were slightly increased compared to controls (Figure 5D and *Online Supplementary Figure S2A*). Gating these subsets into a rainbow plot based on their ploidy showed that the increase in smaller megakaryocytes in the *Gfi1b* knockout mice was primarily due to an increase in cells of the 2N and 4N subsets (Figure 4E). Conversely, the 16N and 32N fractions were decreased in megakaryocytes from *Rosa*-Cre-ERT Gfi1b$^{fl/fl}$ mice, while low-ploidy megakaryocytes represented the vast majority of the smaller cells seen in the *Gfi1b* knockout mice (Figure 4D,

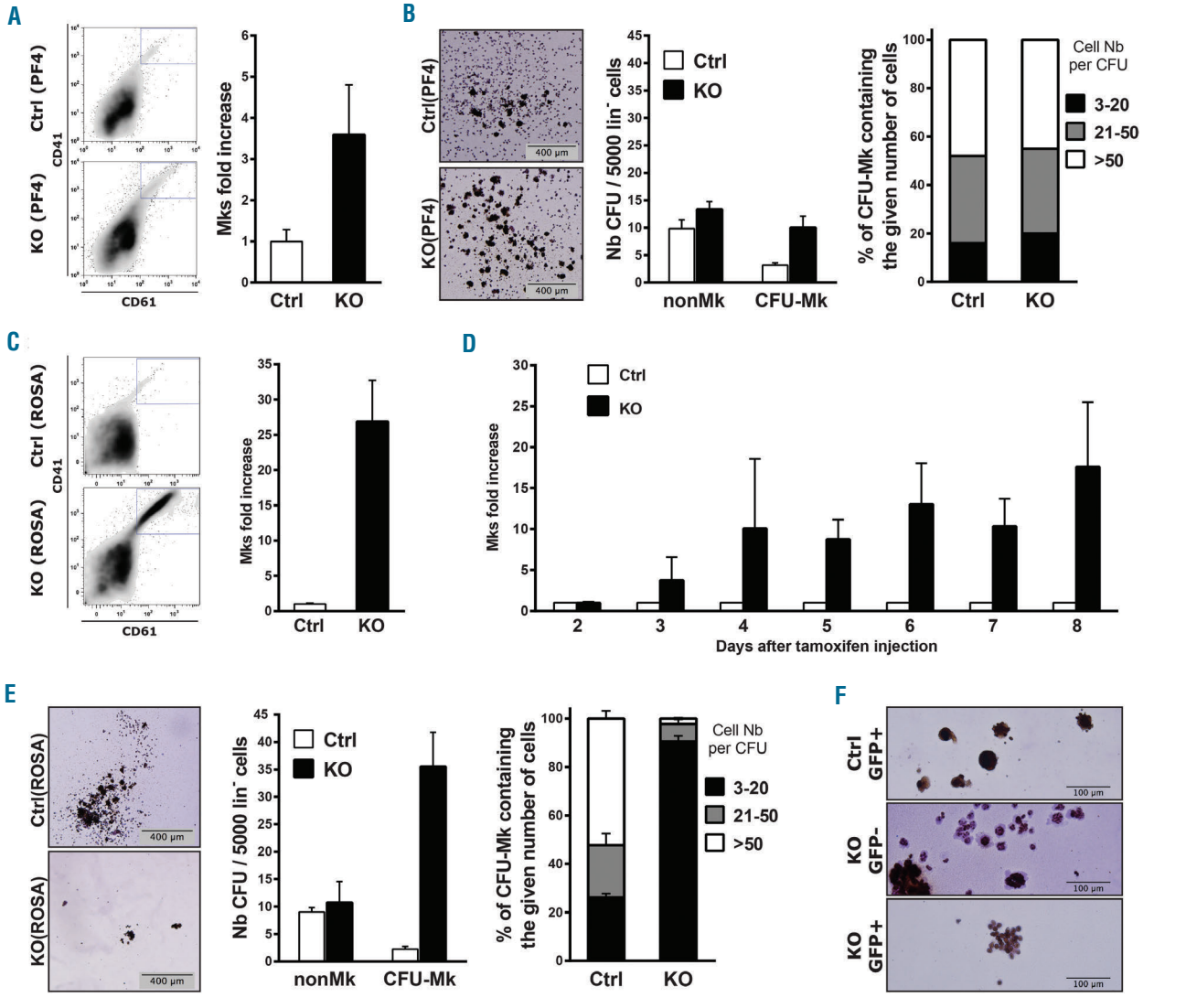

Figure 3. Megakaryocytic dysplasia associated with the loss of GFI1B in the total bone marrow or specifically in megakaryocytes. (A) Representative FACS plot and quantitation of the bone marrow lin$^-$ cKit$^+$CD41$^+$CD61$^+$ megakaryocyte expansion in *Pf4*-cre *Gfi1b*$^{fl/fl}$ animals (n = 11) compared to controls (n = 23). Values were normalized to matching controls and reported as mean ± SD. Student *t*-test with Welch correction: *P*<0.0001. (B) Collagen-based CFU-Mk assay of lineage-negative bone marrow cells: 5,000 to 10,000 lineage-depleted cells from *Pf4*-Cre *Gfi1b*$^{fl/fl}$ knockout (n = 3) or 15,000 lineage-depleted cells from *Pf4*-Cre *Gfi1b*$^{wt/fl}$ control mice (n = 3) were plated on collagen and allowed to grow for 7 days. Colonies were stained for acetylcholinestrase (AChE) activity and counted. Colonies staining AChE-positive were counted as CFU-Mk whereas AChE-negative colonies were counted as non-megakaryocyte CFU. In addition, the CFU-Mk were scored according to the number of cells they contained and sorted in three categories (3-20 cells; 21-50 cells; and >50 cells). Nb: number; Mk: megakaryocytes. (C-D) Representative FACS plot and quantitation of the bone marrow megakaryocyte expansion in *Rosa*-Cre-ERT *Gfi1b*$^{fl/fl}$ (n = 5) compared to controls (n = 4) 2 months after tamoxifen injection (C; Student *t*-test with Welch correction: *P*=0.0024) and kinetics of megakaryocyte expansion upon tamoxifen injection (D). In both experiments, values were normalized to sex- and age-matched controls and reported as mean ± SD. (E) Collagen-based CFU-Mk assay of lineage-negative bone marrow cells from *Rosa*-Cre-ERT *Gfi1b*$^{fl/fl}$ mice (n = 3) and control mice (n = 3) were plated on collagen and colonies were assessed as in (B). (F) Collagen-based CFU-Mk assay done on sorted lin$^-$cKit$^+$ (LK) GFP$^+$ and LK GFP$^-$ cells from *Rosa*$^{mT/mG}$ *Rosa*-Cre-ERT *Gfi1b*$^{wt/fl}$ (Ctrl) and *Rosa*$^{mT/mG}$ *Rosa*-Cre-ERT *Gfi1b*$^{fl/fl}$ (KO) animals treated with tamoxifen 2 months prior to the experiment. In this setting, GFP$^+$ cells are derived from progenitors/stem cells in which the Cre was activated through tamoxifen treatment, whereas the GFP$^-$ cells are cells deriving from progenitor/stem cells that escaped Cre activation upon tamoxifen treatment.

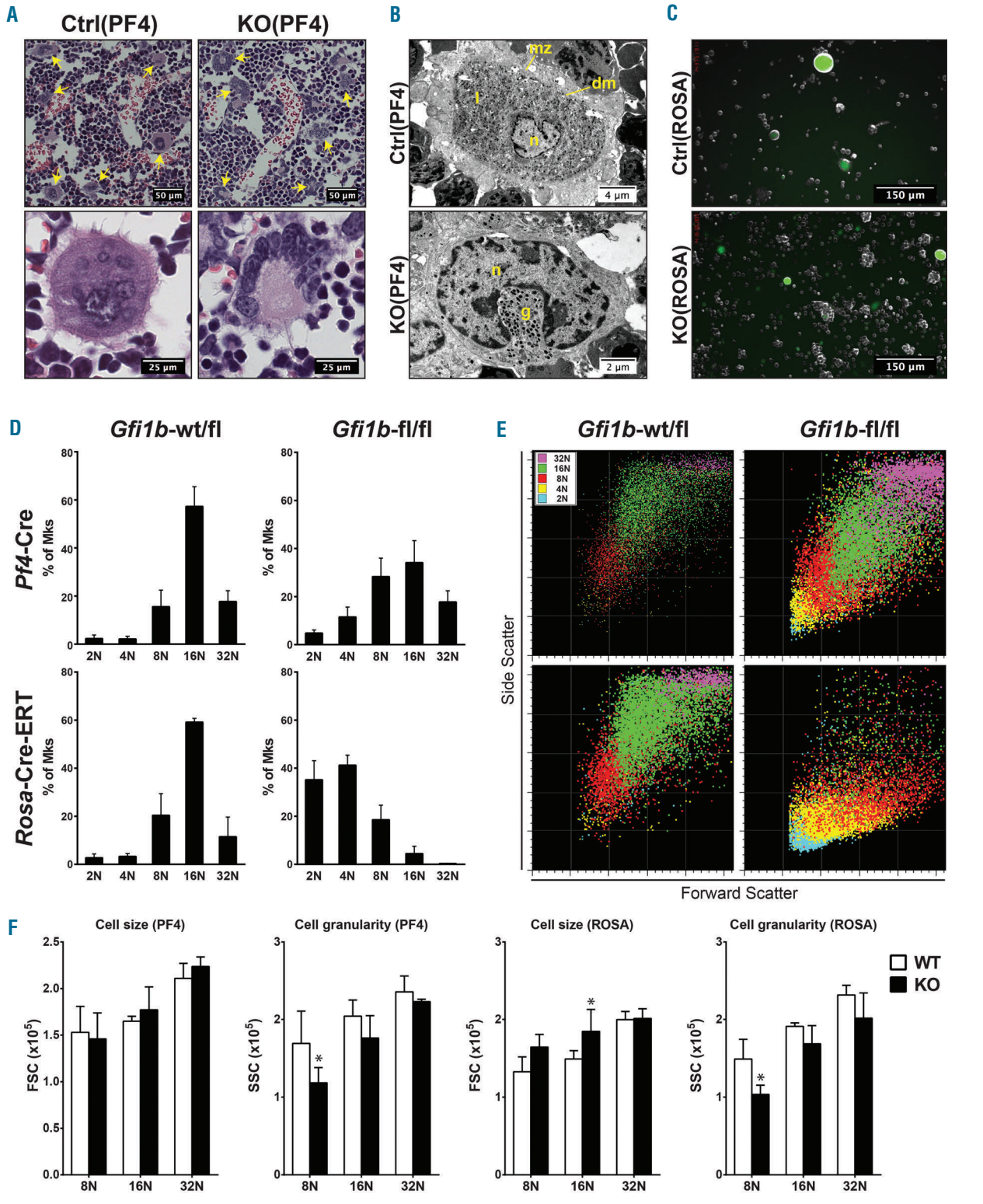

Figure 4. Abnormal nuclear organization, cell size and ploidy of *Gfi1b*-null megakaryocytes. (A) Hematoxylin and eosin staining of bone section from *Pf4*-Cre *Gfi1b*$^{wt/fl}$ (Ctrl) and *Pf4*-Cre *Gfi1b*$^{fl/fl}$ (KO) mice shown at 40X and 100X showing abnormal staghorn-shaped polylobulated nuclei in the *Gfi1b*-null megakaryocytes compared to controls. Arrows indicate megakaryocytes. (B) Transmission electron microscopy of a bone section from *Pf4*-Cre *Gfi1b*$^{wt/fl}$ (Ctrl; magnification: 1400x) and *Pf4*-Cre *Gfi1b*$^{fl/fl}$ (KO; 2900x) mice. In control megakaryocytes, the marginal zone (mz), the demarcation membrane (dm) and the intermediate zone (l) rich in granules are well defined, whereas in knockout megakaryocytes, these structures are poorly defined with the granules (g) often restricted to a single zone of the cytoplasm (in this case within the pocket formed by the nucleus (n). (C) Superimposition of a dark field and fluorescence microscopy of a culture in suspension of primary megakaryocytes derived from *Rosa*-Cre-ERT *Gfi1b*$^{wt/EGFP}$ (Ctrl) and *Rosa*-Cre-ERT *Gfi1b*$^{fl/EGFP}$ (KO) mice showing the presence of a large number of smaller green cells in the knockout that are completely absent in the control culture which shows only larger green cells. (D) Quantification of the ploidy in the most mature megakaryocyte population (defined as being Lin$^-$ cKit$^+$ CD9^{hi} CD41^{hi} CD61^{hi}) in both *Pf4*-Cre and *Rosa*-Cre-ERT-driven *Gfi1b* knockouts 2 months after Cre induction (n = 4 for each group) and given as the mean percentage of the total megakaryocytes ± SD. (E) Megakaryocyte rainbow plots produced by back-gating the cells based on their ploidy on the forward scatter (FSC)/side scatter (SSC) plot. (F) Comparison of the FSC (cell size) and SSC (cell granularity) of the polyploid cell populations (8N, 16N and 32N) of the cells analyzed in (D). The bar graphs present the mean ± SD. The means were compared using a Student *t*-test corrected for multiple comparisons using the Sidak-Bonferroni method. (*) $P \leq 0.01$.

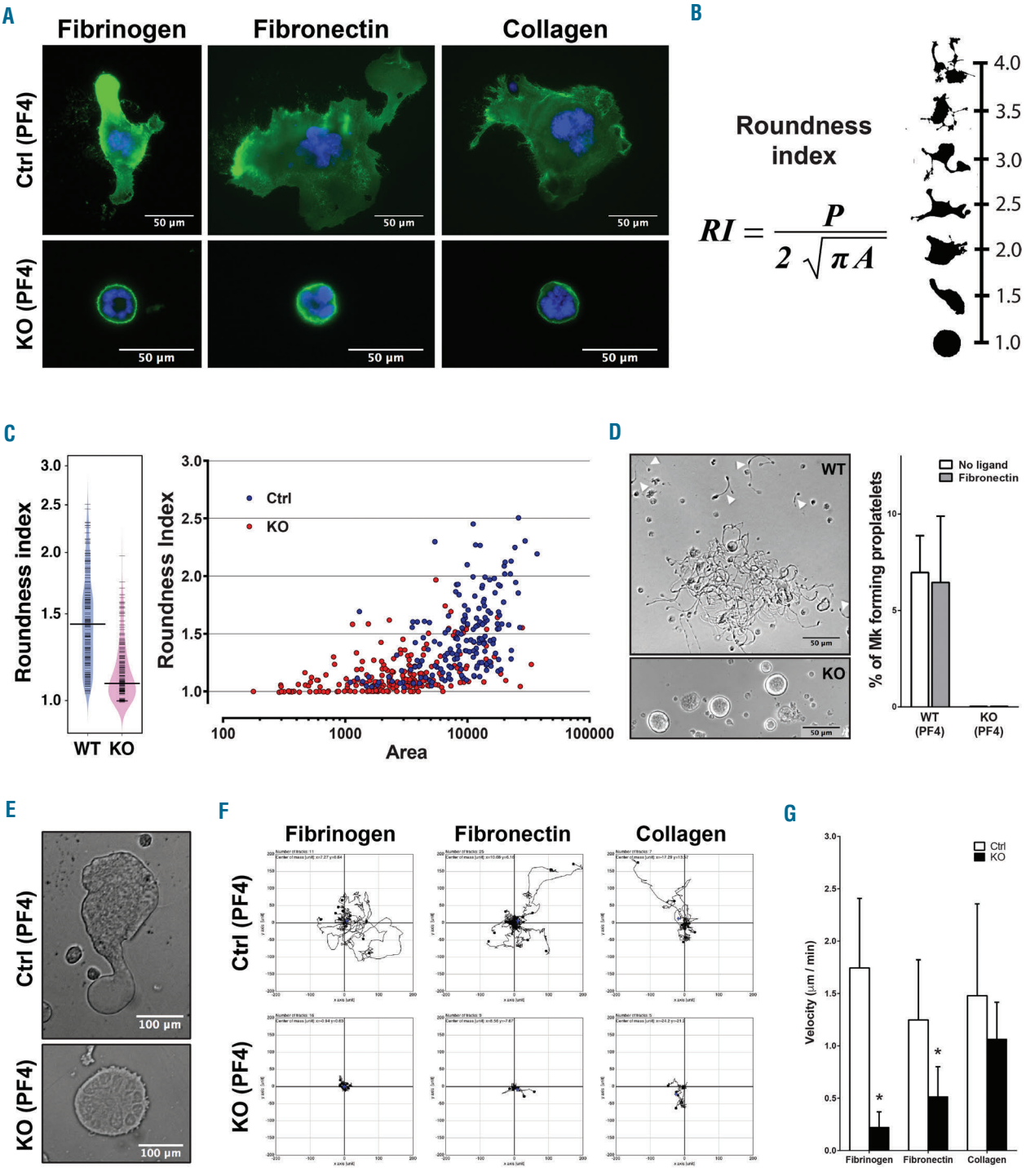

Figure 5. Impaired response to integrin receptors' ligands in GFI1B-deficient megakaryocytes. (A) Primary megakaryocyte cultures derived from *Pf4*-Cre *Gfi1b*$^{fl/fl}$ mice and control mice were plated on slides coated with collagen, fibronectin or fibrinogen, allowed to spread for 5 h, then fixed and stained with DAPI and FITC-CD41 antibody. (B) To assess the responsiveness of megakaryocytes that spread on coated slides more quantitatively, we first measured their individual periphery (P) and area (A), then divided these peripheries by the circumference of perfect circles of the same area. This ratio, or Roundness Index (RI), gives a quantitative value that is directly proportional to the structural complexity of the cells regardless of their cytoplasmic mass. As visual comparative examples, the shapes of cells with defined RI are presented next to the scale for clarity. (C) RI of *Pf4*-Cre *Gfi1b*$^{fl/fl}$ knockout- or *Pf4*-Cre *Gfi1b*$^{wt/fl}$ control-derived megakaryocytes spread on fibronectin and plotted as bean plots as well as against their cellular area showing that the RI of *Gfi1b*-null megakaryocytes remains low even as cell size increases. Mann-Whitney *U*-test: $P<0.0001$. (D) Assessment of the capacity of *Pf4*-Cre *Gfi1b*$^{fl/fl}$ knockout- (KO) or *Pf4*-Cre *Gfi1b*$^{wt/fl}$ control-derived (WT) megakaryocytes to produce proplatelet formation and platelet release in vitro. Proplatelet-forming megakaryocytes were identified by light microscopy and counted along non-proplatelet megakaryocytes (rounded shape) and plotted as a percentage of total megakaryocytes. The presence of platelet-like structure (white arrows) was also assessed but not quantified. While proplatelets and platelets were present in all wild-type cultures, they were never observed in GFI1B-deficient megakaryocytes (KO). The bar graph presents the mean ± SD of four independent experiments (n = 4 for each condition). (E) Still images extracted from a time-lapse microscopy in phase contrast recorded over several hours (see *Online Supplementary Videos* S1 and S2) of *Pf4*-Cre *Gfi1b*$^{fl/fl}$ knockout- or *Pf4*-Cre *Gfi1b*$^{wt/fl}$ control-derived megakaryocytes plated on fibronectin. (F-G) The motility of *Pf4*-Cre *Gfi1b*$^{fl/fl}$ knockout- or *Pf4*-Cre *Gfi1b*$^{wt/fl}$ control-derived megakaryocytes was assessed by time-lapse microscopy over several hours upon plating on fibrinogen (Ctrl: n = 11; KO: n = 16), fibronectin (Ctrl: n = 25; KO: n = 9) and collagen (Ctrl: n = 6; KO: n = 5). Single megakaryocytes were manually tracked using the cell centroid position and their path recorded (F), allowing calculation of their average velocity during the course of the experiment. The results are presented as mean velocity ± SD in µm per minute (G). Student *t*-test: (*) marks statistical significance ($P<0.0001$). Videos from (F) can be seen in the *Online Supplementary Material* (*Videos S3-S8*).

E and *Online Supplementary Figure S2*). Megakaryocytes with the same ploidy from *Gfi1b*-null mice had the same size (forward scatter) as controls and a tendency to a have lower mean side scatter (Figures 4F and *Online Supplementary Figure S2B*).

Defective integrin signaling and cellular spreading of *Gfi1b*-null megakaryocytes

When grown on integrin-specific ligands, megakaryocytes start to spread by forming large lamellipodia that depend on the interaction between extracellular matrix components and integrins.[20] To assess how Gfi1b affects this process, we cultured megakaryocytes from either *Pf4*-Cre *Gfi1b*$^{fl/fl}$ or control mice on fibronectin, fibrinogen or collagen. Control megakaryocytes were able to form lamellipodia and filopodia-like protrusions on collagen (a ligand for the $\alpha_2\beta_1$ integrin), fibronectin (a ligand for $\alpha_{IIb}\beta_3$ and $\alpha_v\beta_1$) and fibrinogen (a ligand for $\alpha_{IIb}\beta_3$ and $\alpha_v\beta_3$),[21] whereas GFI1B-deficient megakaryocytes were unable to do so and maintained a spherical shape (Figure 5A).

To exclude the possibility that this low response of GFI1B-deficient cells to integrin ligands was simply due to their smaller size, we established a method to measure response to integrin ligands independently of cell size. By comparing the periphery of each cell that attached to a ligand in culture to the circumference of a perfect circle ($2\pi r$) with the same area, we calculated a "roundness index" (RI) resulting in a numerical value that increases as the complexity of a spreading cell increases, starting at RI=1 for a perfectly round cell (Figure 5B). A comparison of the RI of cultured cells clearly showed that GFI1B-deficient megakaryocytes maintained significantly low RI and were unable to spread, suggesting a poor response to integrin ligands. This defect was independent of their size (Figure 5C) or their state of maturity (*Online Supplementary Figure S3A,B*), ruling out that the poor responsiveness could be due to a smaller cytoplasm or to an immature state. Time-lapse video microscopy on live cells confirmed a severe impairment of motility of GFI1B-deficient megakaryocytes in response to fibronectin and fibrinogen and to a lesser extent to collagen (Figure 5E-G; *Online Supplementary Videos S1-S8*) also independently of the state of maturity (*Online Supplementary Figure S3C*).

The lower ploidy of most *Rosa*-Cre-ERT *Gfi1b*$^{fl/fl}$ megakaryocytes suggests an immature state or, at the very least, defective endomitosis and could provide an explanation for the absence of platelet production. However, the observation that, in *Pf4*-Cre *Gfi1b*$^{fl/fl}$, megakaryocytes can fully mature but still cannot produce platelets (Figure 5D) indicates that loss of GFI1B inhibits proplatelet formation in mature megakaryocytes.

GFI1B controls actin polymerization and microtubule organization

We next examined how GFI1B deficiency affected events downstream of integrin receptors, such as actin polymerization in megakaryocytes that were allowed to spread on fibronectin. In contrast to control megakaryocytes, which became highly positive for F-actin, Gfi1b-deficient megakaryocytes displayed lower levels of actin filaments with a 3-fold reduction of fluorescence intensity despite the fact that the expression of un-polymerized actin was not affected in the knockout (Figure 6A,C,G). Assessment by immunofluorescence of β-tubulin in megakaryocytes spread on fibronectin revealed that *Gfi1b*-null megakaryocytes seemed unable to produce fibers of microtubules (Figure 6B), although quantitation of fluorescence intensity showed only a mild, albeit significant, reduction of β-tubulin in GFI1B-deficient megakaryocytes compared to controls (Figure 6D). Measurements of fluorescence intensity across a horizontal section passing through the center of each cell showed that the intracellular localization of β-tubulin was altered in *Gfi1b*-null megakaryocytes (Figure 6E). In controls, the tubulin network was found to be positioned both at the center of the cell and at the cellular cortex as a ring of clearly defined microtubule fibers characteristic of later stages of maturation.[22] In contrast, in GFI1B-deficient megakaryocytes, β-tubulin was retained in the center of the cells, within a pocket formed by the ring-shaped nucleus, seemingly failing to polymerize into microtubules, and this, independently of the maturation state (Figure 6B,E and *Online Supplementary Figure S3D* and *Online Supplementary Video S9*), indicating either a profound defect in microtubule polymerization or a failure of GFI1B-deficient megakaryocytes to get activated by fibronectin. However, analysis of both α- and β-tubulin by western blot revealed that while the β-tubulin content was not altered significantly in the knockout, α-tubulin, on the other hand, was dramatically reduced to almost undetectable levels, including its acetylated form and even upon phorbol myristate acetate activation (Figure 6G). Importantly, the lack of responsiveness to integrin-specific ligands observed in *Gfi1b*-null megakaryocytes was not due to the absence of the proper integrin receptors, which were either unaffected or increased in the knockout when measured by FACS (Figure 6D and *Online Supplementary Figure S4*) or by immunoblotting (Figure 6G). Interestingly, subpopulations of megakaryocytes defined by their integrin signature were only marginally affected in the *Gfi1b* knockout mice compared to the wild-type ones (*Online Supplementary Figure S5*).

Expression profiling of megakaryocytes from both *Pf4*-Cre- and *Rosa*-Cre-ERT-driven *Gfi1b*-knockout and control mice by RNA-Seq showed a strong correlation between the two models and with a previously published data set obtained from a different *Gfi1b* knockout model[12] (Figure 7A and *Online Supplementary Figure S6*). Genes related to the actin cytoskeleton were found to be deregulated in cells from *Pf4*-Cre *Gfi1b*$^{fl/fl}$ mice but not in megakaryocytes from *Rosa*-Cre *Gfi1b*$^{fl/fl}$ mice (Figure 7B and *Online Supplementary Figure S6C*). However, in both models, genes with deregulated expression in GFI1B-deficient megakaryocytes were enriched in categories defined by signaling through Rho GTPases and regulation of microtubules (Figure 8B,C and *Online Supplementary Figure S7A,B*). Notable exceptions are the α-tubulin genes, which were downregulated in both knockouts (Figure 7C). Also, many progenitor-specific and megakaryocyte-specific genes, such as *Kitlg*,[23] *Il6*[24] *Itgb3*,[20] *CD9*,[25] and *Mpl*,[26] were up-regulated in *Gfi1b*-null megakaryocytes (*Online Supplementary Figure S7C*). However, genes from the "hematopoietic lineage" gene set were not enriched in cells from *Pf4*-Cre *Gfi1b*$^{fl/fl}$ mice, but showed a strong negative regulation in *Rosa*-Cre-ERT *Gfi1b*$^{fl/fl}$ animals (*Online Supplementary Figure S7C*), suggesting that megakaryocytes from *Rosa*-Cre-ERT *Gfi1b*$^{fl/fl}$ mice have a more immature/progenitor-like phenotype. Conversely, a "megakaryocyte differentiation" gene set based on the paper by Lim *et al.*[27] showed a strong enrichment in cells from the *Pf4*-Cre-driven *Gfi1b* knockout mice but not in

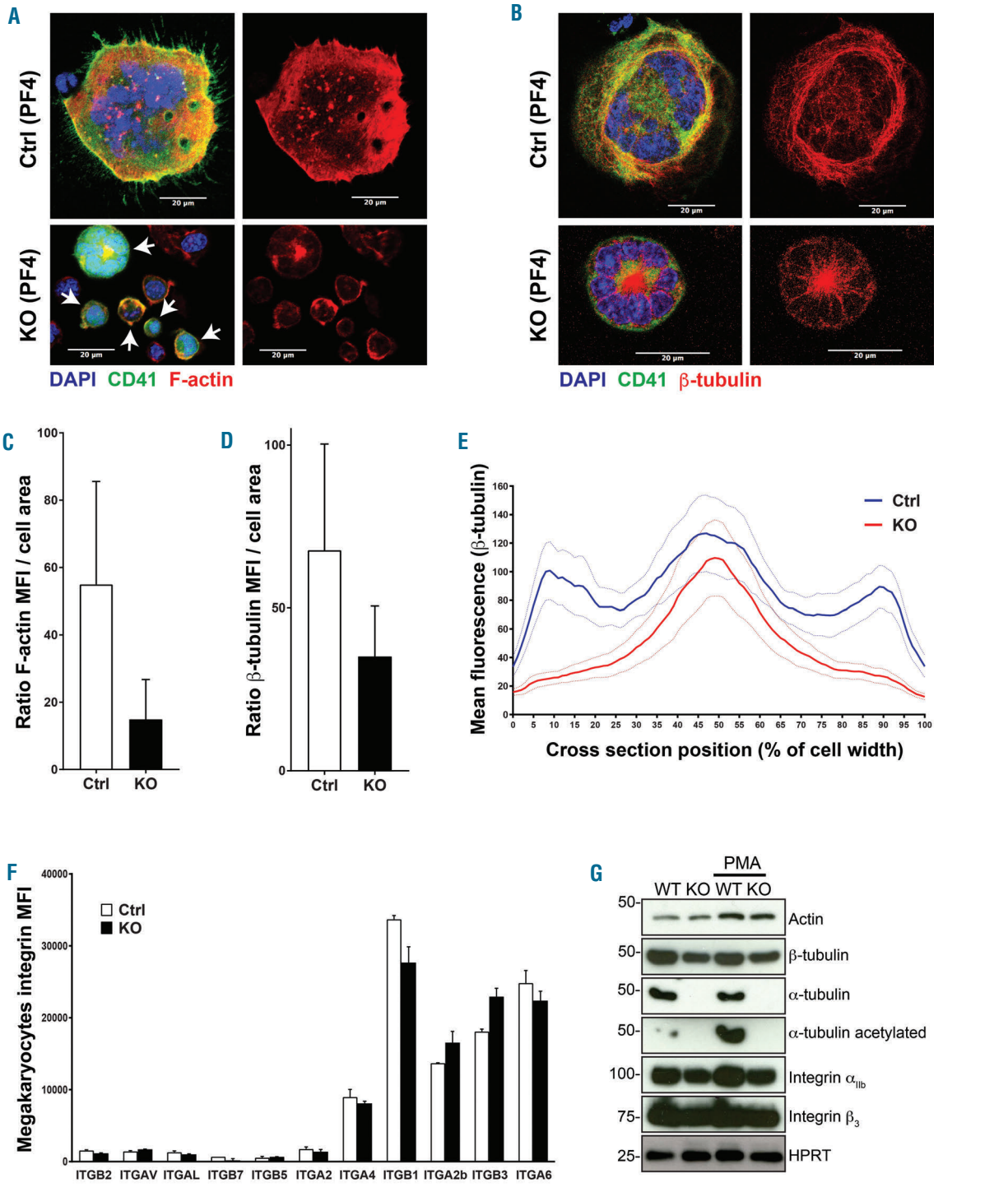

Figure 6. Defect in cytoskeleton organization in *Gfi1b*-null megakaryocytes. (A) *Pf4*-Cre *Gfi1b*$^{fl/fl}$ knockout megakaryocytes (KO; n = 188) or control megakaryocytes (Ctrl; n = 30) were plated on fibronectin in a single 12-µ-Chambers slide to minimize variation between samples and, after fixing, labeled with a FITC-conjugated anti-CD41 antibody and AF555-conjugated phalloidin to measure actin fibers. Pictures were taken by fluorescent microscopy and the mean fluorescence intensity was measured and plotted against the cell size defined as the area covered on the coated slide. Megakaryocyte enrichment on a bovine serum albumin gradient also allows for some non-megakaryocyte CD41$^-$ cells to be present. Therefore, to avoid confusion because of the relative small cell size, CD41$^+$ megakaryocytes are identified with arrows in the knockout. (B) Cells from *Pf4*-Cre *Gfi1b*$^{fl/fl}$ knockout (KO; n = 70) or control (Ctrl; n = 41) mice were plated on fibronectin as in (A) and were stained with an AF555-conjugated anti-β-tubulin antibody to show general intracellular distribution of β-tubulin, which showed poor polymerization in the knockout compared to controls. (C) The mean fluorescence intensity (MFI) of F-actin from (A) was measured and the ratio (MFI/cell area) was calculated and presented as mean ± SD. Student *t*-test with Welch correction: $P<0.0001$. (D) The mean fluorescence intensity of β-tubulin from (B) was measured and the ratio (MFI/cell area) was calculated and presented as mean ± SD. Student *t*-test with Welch correction: $P<0.0001$. (E) Analysis of a cross-section passing through the center of 30 megakaryocytes (n = 30) per genotype [*Pf4*-Cre *Gfi1b*$^{flox/flox}$ (KO) and *Pf4*-Cre *Gfi1b*$^{flox/wt}$ (Ctrl) mice coming from (B and D)]. The diameter was subdivided into 100 sections, each representing 1% of the cell width and the AF555 intensity was measured at each of these sections with section 0 starting at one side and section 100 ending at the other side. This intensity was then plotted as mean ± CI along the whole cell section. (F) Integrin receptors present at the surface of lin$^-$cKit$^+$Cd41$^+$CD61$^+$ megakaryocytes from Pf4-Cre *Gfi1b*$^{fl/fl}$ knockout (KO) mice were assessed by FACS and their MFI was compared to that of *Pf4*-Cre *Gfi1b*$^{wt/fl}$ control (Ctrl) animals and presented as mean ± SD (n = 2 for both genotypes). (G) Immunoblot detection of megakaryocyte cytoskeleton proteins (actin, β-tubulin, α-tubulin and the acetylated form of α -tubulin) and the two subunits of the megakaryocyte-specific fibrinogen/fibronectin integrin receptor $\alpha_{IIb}\beta_3$ in megakaryocytes derived from the bone marrow from *Pf4*-Cre *Gfi1b*$^{flox/flox}$ (KO) and *Pf4*-Cre *Gfi1b*$^{wt/wt}$ (WT) mice with or without phorbol myristate acetate (PMA) activation. HPRT is used as a loading control. This experiment was repeated at least three times with consistent results.

cells from the *Rosa*-Cre-ERT deleted animals (*Online Supplementary Figure S7D*), suggesting that megakaryocytes were more differentiated in the *Pf4*-Cre model than in the *Rosa*-Cre model. Interestingly, many genes from the microtubule pathways that were up-regulated in *Gfi1b*-null cells belonged to the Rho guanine nucleotide exchange factors (ArhGEF) gene family (Figure 7D and *Online Supplementary Figure S7B*). Western analysis revealed a dramatic increase of both the total and the phosphorylated form of PAK4, a key player in the regula-

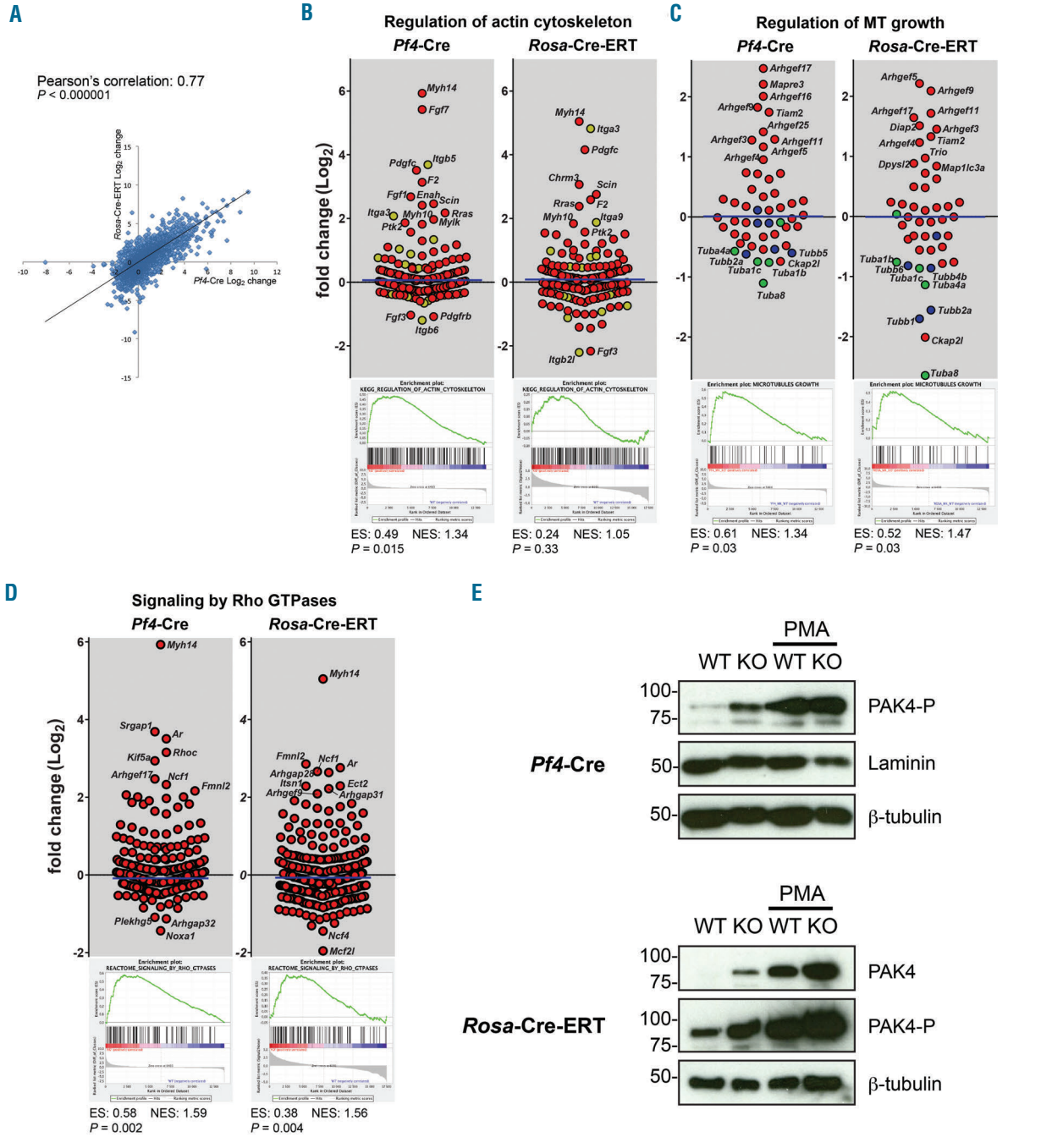

Figure 7. Gene expression profiling in *Gfi1b*-null megakaryocytes reveals defects in cytoskeleton regulation pathways. (A) Correlation between the gene expression profiles from the RNA-Seq on *Pf4*-Cre- and *Rosa*-Cre-ERT-driven *Gfi1b* knockout. The Pearson coefficient is shown. The *P* value was determined using a permutation test with $1x10^6$ re-samplings. (B-D) Gene set enrichment analysis (GSEA) of cytoskeleton-related functions on RNA-Seq expression profiles from both *Pf4*-Cre *Gfi1b*$^{fl/fl}$ and *Rosa*-Cre-ERT *Gfi1b*$^{fl/fl}$ (+ tamoxifen) megakaryocytes. Data from knockout cells were compared with their respective *Pf4*-Cre *Gfi1b*$^{wt/fl}$ and *Rosa*-Cre *Gfi1b*$^{wt/fl}$ (+ tamoxifen) controls. Above, genes are plotted based on their expression fold change (log_2 scale) and for each of these gene sets, the top over-expressed and under-expressed genes are identified on the dot plot. (B) Actin cytoskeleton regulation pathway with integrin genes highlighted with a yellow color . (C) Microtubule growth pathway in which the tubulin genes are highlighted in blue (β-tubulin family) and in green (α-tubulin family). (D) Signaling by RHO GTPase gene set. Normalized enrichment scores (NES) and nominal *P*-values (*P*) are given for each GSEA plot. (E) Immunoblot detection of the phosphorylated form of PAK4 (also recognizes the other type II PAKs, PAK5 and PAK6) in megakaryocytes derived from the bone marrow of *Pf4*-Cre *Gfi1b*$^{flox/flox}$ (KO) and *Pf4*-Cre *Gfi1b*$^{wt/wt}$ (WT) mice (top) and *Rosa*-Cre-ERT *Gfi1b*$^{flox/flox}$ (KO) and *Rosa*-Cre-ERT *Gfi1b*$^{wt/wt}$ (WT) mice (bottom) with or without phorbol myristate acetate (PMA) activation and using β-tubulin and/or laminin as loading controls. This experiment was repeated at least three times with consistent results.

tion of both actin and tubulin cytoskeletons, suggesting that hyperactivation of the integrin signaling through PAK might be responsible for the phenotype.

The spreading defects of *Gfi1b*-null megakaryocytes can be partially rescued by inhibitors of integrin signaling and fully rescued by a pan-p21 activated kinase inhibitor *in vitro*

To functionally verify the results obtained from the RNA-Seq analysis, which suggested that integrin signaling might be hyper-activated in the knockout, we used small molecule inhibitors against FAK (PF573228), PAK (PF3758309 and FRAX486), ROCK (Y27632), CDC42 (ML141), RAC1-GEF interaction (NSC 23766 and W56) and myosin II (Blebbistatin). Megakaryocytes were allowed to spread for 5 h on fibronectin in the presence or absence of the inhibitors and the RI was measured on $CD41^+$ cells (Figure 8A and *Online Supplementary Figure S8A,B*). A partial rescue of the Gfi1b null phenotype was observed in the presence of either PAK (FRAX486), FAK, ROCK and RAC1 (W56) inhibitors. The strongest effect and a full rescue was obtained with the pan-PAK inhibitor (PF3758309). The RI for the PF3758309-treated *Gfi1b* knockout megakaryocytes were undistinguishable from those of PF3758309-treated wild-type megakaryocytes, which themselves spread better than the untreated wild-type control megakaryocytes (Figure 8A,B). These cells also exhibited an improved β-tubulin distribution at the apex of the cells (Figure 8C) and their motility improved to a level undistinguishable from that of the controls (Figure 8D). However, none of the inhibitors used was able to rescue the *in vitro* proplatelet production defect of *Gfi1b*-null megakaryocytes; rather, inhibition of PAK with either PF3758309 or FRAX486 led to the death of megakaryocytes (both wild-type and knockout) over the time-course necessary for cells to produce proplatelets (Figure 8D).

Discussion

Deleting *Gfi1b* by *Pf4*-Cre at later stages of megakaryocyte differentiation or by *Rosa*-Cre-ERT in the entire hematopoietic lineage and thus also before megakaryocyte commitment produced a phenotype that resembles the one seen in patients with *GFI1B*-related thrombocytopenia with rare, larger platelets.[4,5] Upon deletion of *Gfi1b* by Cre induction in adult bone marrow cells via tamoxifen, we observed defects in the earliest stages of megakaryocyte maturation, with a majority of cells that failed to undergo proper endomitosis or to form large CFU-Mk colonies, suggesting a block in megakaryocyte maturation/differentiation. In contrast, inactivation of *Gfi1b* at later stages of megakaryocyte differentiation via a *Pf4*-Cre transgene resulted in only mild defects in polyploidization or CFU-Mk colony formation, but still abrogated platelet production completely, suggesting that in this case, the defect lies in the terminal process of proplatelet formation and platelet release, demonstrating that *Gfi1b* plays a role in both megakaryocyte differentiation and platelet production. The role of *Gfi1b* in this terminal process is also supported by the observation that platelet release is arrested very rapidly after tamoxifen injection in *Rosa*-Cre-ERT $Gfi1b^{fl/fl}$, before the block in megakaryocyte differentiation could lead to exhaustion of mature megakaryocytes. It has been shown that large platelets and circulating megakaryocyte fragments can be consequences of insufficient membrane- or aberrant organelle structure of megakaryocytes,[16] which could provide an explanation for the presence of these features in *Gfi1b*-knockout mice. The presence of rare, large platelets despite the incapacity of megakaryocytes to form proplatelets suggests the existence of an alternative albeit less efficient mechanism such as fragmentation of megakaryocyte cytoplasm in pulmonary capillaries.[28]

Previous studies have shown that several integrins are deregulated in *Gfi1b*-null cells[5,12,13] and our RNA-Seq data confirm these observations. Expression of the megakaryocyte-specific integrin β_3 (*Itgb3*) is up-regulated in our models and this higher expression leads to the expected increase of the megakaryocyte-specific integrin α_{IIb}/β_3 complex at the cell surface.[29] Because the α_{IIb}/β_3 complex is the main receptor for fibrinogen[30] and fibronectin,[31] it was surprising that the *Gfi1b*-null megakaryocytes were not responsive to these two ligands. Conversely, the main collagen receptor ($\alpha_2\beta_1$ integrin)[32] is present on *Gfi1b*-null megakaryocytes at lower levels than controls, but the cells still had a defective response. Hence, the deregulation of integrin receptors alone cannot explain the poor responsiveness of *Gfi1b*-null megakaryocytes, although it has been reported that abnormal activation of the α_{IIb}/β_3 complex can lead to defective proplatelet formation.[33] It is rather likely that elements of the intracellular integrin signaling pathways responsible for cell spreading and motility and for megakaryocyte activation are disrupted in the absence of GFI1B. The poor response to integrin activation in *Gfi1b*-null megakaryocytes supports this notion.

Remodeling of cytoskeleton components is involved in the two cellular processes that are most affected in *Gfi1b* knockout megakaryocytes: endomitosis and platelet release. Polyploidization that occurs through endomitosis is dependent on the regulation of an atypical multipolar mitotic spindle that, in addition to a failed cleavage furrow formation in late anaphase, leads to the abortion of both cytokinesis and karyokinesis.[34,35] Similarly, regulation of microtubules is essential for proplatelet formation[22,36,37] and given that megakaryocytes from *Pf4*-Cre $Gfi1b^{fl/fl}$ mice, which exhibit an almost normal polyploidization, are unable to produce platelets, a failure to assemble, organize or stabilize microtubules, as was observed with megakaryocytes with disorganized β-tubulin that were unable to form visible microtubule fibers, is likely one of the main defects in *Gfi1b*-null megakaryocytes. We have shown that this profound defect can be explained by the incapacity of β-tubulin to polymerize into microtubules due to the lack of α-tubulin.

On the other hand, cellular motility and spreading, which are also profoundly defective in *Gfi1b*-null megakaryocytes, rely essentially on the actin cytoskeleton dynamics through integrin signaling. Interestingly, the fact that these defects are seen regardless of the level of maturation in the *Pf4*-driven *Gfi1b* knockout argues against the possibility that these defect could be solely due to a block of maturation.

The expression of genes coding for several components involved in the organization of both actin and tubulin cytoskeleton, for instance several small GTPases of the Rho family as well as Rho guanine nucleotide exchange factors (ArhGEF), was deregulated in *Gfi1b*-null megakaryocytes. Our experiments with small molecule inhibitors have identified integrin signaling pathway

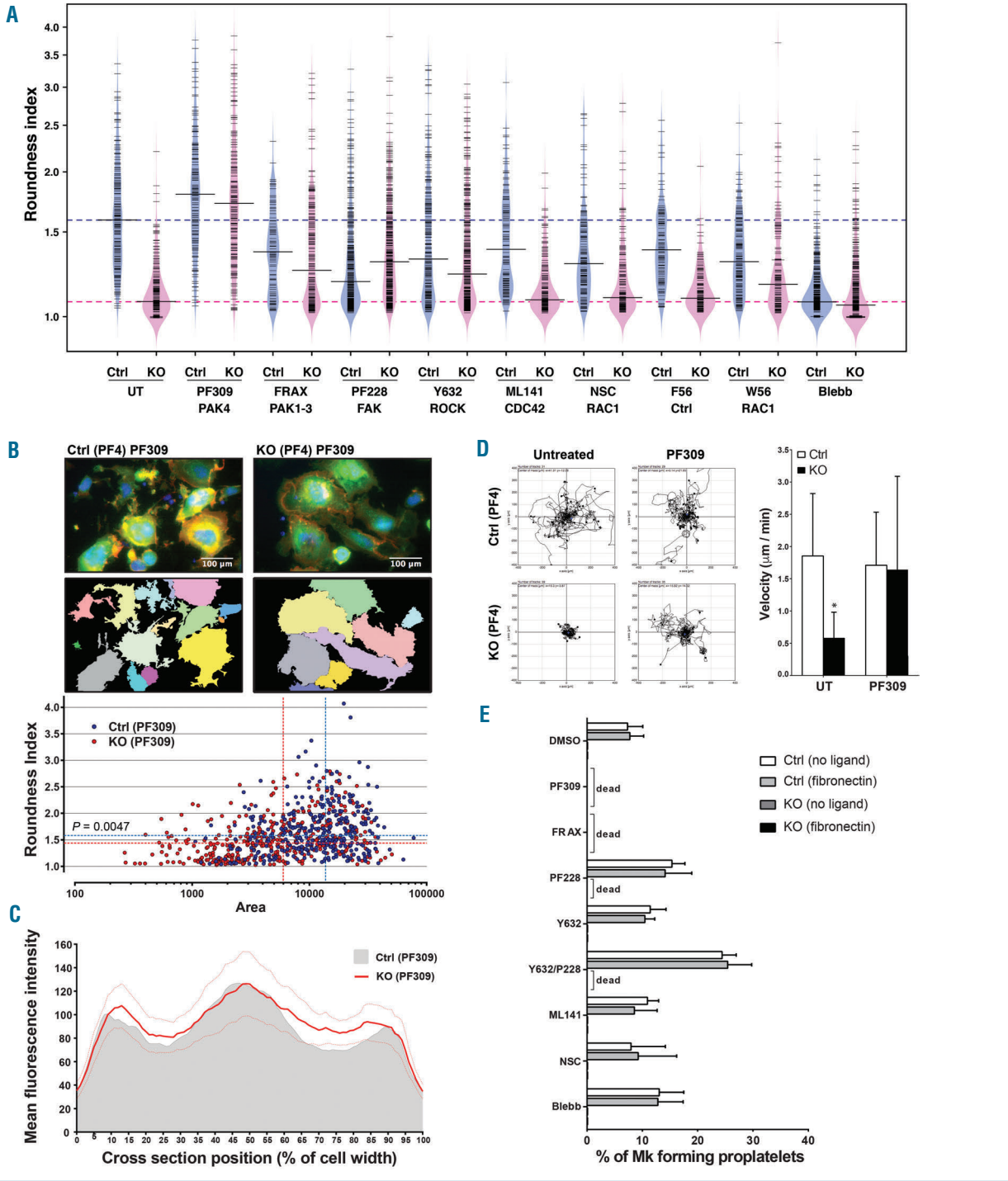

Figure 8. Cytoskeleton rescue by a PAK inhibitor. (A) Megakaryocytes from *Pf4*-Cre *Gfi1b*$^{wt/fl}$ (Ctrl) and *Pf4*-Cre *Gfi1b*$^{fl/fl}$ (KO) mice were allowed to spread on fibronectin for 3 h in the absence (UT; KO: n = 430; Ctrl: n = 361) or presence of different inhibitory small molecules: PF3758309 (PF309; PAK4 inhibitor; KO: n = 184; Ctrl: n = 147); FRAX486 (FRAX; PAK1-3 inhibitor; KO: n = 220; Ctrl: n = 93); PF573288 (PF228; FAK inhibitor; KO: n = 405; Ctrl: n = 353); Y27632 (Y632; ROCK inhibitor; KO: n = 396; Ctrl: n = 223); ML141 (CDC42 inhibitor; KO: n = 169; Ctrl: n = 123); NSC23766 (NSC; RAC1 inhibitor; KO: n = 153; Ctrl: n = 136); F56 (control peptide; KO: n = 142; Ctrl: n = 107); W56 (RAC1 inhibitor; KO: n = 146; Ctrl: n = 152); and blebbistatin (Blebb; myosin II inhibitor; KO: n = 424; Ctrl: n = 395). The roundness index (RI) of these cells was scored as in Figure 6B and presented as beanplots comparing the median for all conditions. A Kruskal-Wallis one-way analysis of variance done on these data and followed by a Dunn post-hoc multiple comparison test revealed a highly significant difference ($P<0.0001$) between the samples' median; the Dunn test identifies significant differences between the untreated KO megakaryocytes and the KO megakaryocytes treated with the PAK inhibitors PF3758309 and FRAX486, as well as with the RAC1 inhibitor peptide W56. KO megakaryocytes treated with PF3758309 show no statistical difference with untreated or PF3758309-treated control megakaryocytes. (B) Representative microscopy of PF3758309-treated (PF309) control (Ctrl) and knockout (KO) megakaryocytes from (A) stained with DAPI (blue), CD41 (green) and β-tubulin (red) and (top) overlay of all cells present in the field to highlight their spreading (middle). The RI were plotted against their corresponding cell size (bottom). The blue and red dashed lines show the median RI (horizontal) and cell size (vertical) for the control and knockout megakaryocytes, respectively. (C) Cellular distribution of microtubule in knockout megakaryocytes treated with the PAK4 inhibitor PF3758309 (PF309) was analyzed as in Figure 6E and plotted (red line) against the control cells presented in Figure 6E (shaded gray). (D) The motility of *Pf4*-Cre *Gfi1b*$^{fl/fl}$ knockout- or *Pf4*-Cre *Gfi1b*$^{wt/fl}$ control-derived megakaryocytes was assessed by time-lapse microscopy as in Figure 5 in the presence (Ctrl: n = 29; KO: n = 34) or absence (Untreated; Ctrl: n = 31; KO: n = 39) of the PAK4 inhibitor PF3758309 (PF309). The results are presented as mean velocity ± SD in µm per minute. Student *t*-test: (*) marks statistical significance ($P<0.0001$). (E) Megakaryocytes were allowed to form proplatelet-like structures *in vitro* and assessed by light microscopy (as in Figure 5D) in the absence (DMSO) or presence of inhibitors as in (A). Conditions in which cells did not survive over the period of 12 h upon treatment with the inhibitors are labeled as "dead" in the graph. Bar graphs present the mean ± SD of three separate experiments (n = 3).

components as well as PAK, which is targeted by RAC, RHO and CDC42, as two of the critical components affected by GFI1B-deficiency in megakaryocytes. Inhibiting FAK or RHO kinase (ROCK), both important for actin cytoskeleton and integrin signaling,[38,39] led to moderate but significant improvements in the response of *Gfi1b*-null megakaryocytes to integrin ligands and in their capacity to spread on fibronectin. This suggests that aberrant integrin signaling can partially explain the defects of GFI1B-deficient megakaryocytes, an idea supported by a recent study showing a role of GFI1B in the regulation of the integrin-bound proteins Talin1 and Kindlin3.[40]

However, the inhibition of PAK, which regulates both actin cytoskeleton and microtubules through stathmin and GEF-H1,[41,42] by the pan-PAK inhibitor PF-3758309 had the strongest effect on GFI1B-deficient megakaryocytes, completely rescuing their responsiveness to ligands, as shown by their capacity to spread efficiently and their increased motility upon inhibition of PAK. Importantly, even though this PAK inhibitor also had a stimulatory effect on normal megakaryocytes, which spread more efficiently on fibronectin than did the untreated control cells, the responsiveness of the *Gfi1b*-null megakaryocytes was just as good. Because PF-3758309 preferentially inhibits type II PAKs (e.g. PAK4) but lacks specificity,[43] we also used the type I PAK inhibitor FRAX486, which targets PAK1-3,[43] which only mildly rescued the spreading defect. This suggests that GFI1B-deficiency mainly affects signaling through type II PAKs, which is supported by the observation that both the total and the phosphorylated forms of the PAK4 protein are constitutively increased in *Gfi1b* knockout cells. Hence, dysregulation of cytoskeleton dynamics could be the main reason for the absence of the cellular response to several integrin ligands in *Gfi1b*-null megakaryocytes. This is consistent with the up-regulation of ArhGEF in *Gfi1b*-null cells seen in our RNA-Seq experiments, since ArhGEF activate PAK. Because *Pak4* expression is strongly increased in *Gfi1b* knockout cells and since the inhibition of type II PAK restored cellular spreading in the absence of GFI1B, it is conceivable that GFI1B normally inhibits *Pak*. This is further supported by another study that showed that PAK2-deficient megakaryocytes are characterized by an increased polyploidy and an alteration of microtubule organization.[44]

Studies with other transcription factors that are important for proper megakaryopoiesis, such as GATA-1/FOG-1,[45,46] NF-E2 p45,[47] RUNX1[48] and FLI1,[49] have highlighted their multifarious effects that could not all be explained by the deregulation of single pathways. Similarly, we showed that GFI1B is essential for proplatelet formation, but none of the inhibitors used rescued this cell-autonomous process in *Gfi1b*-null megakaryocytes. Confirming previous findings,[50] we also showed that proplatelet formation occurs in the absence of integrin-specific ligands. In this case, the loss of α-tubulin, whose expression might be controlled at least indirectly by GFI1B, and independently of PAK provides an elegant explanation for this phenotype.

Acknowledgments

We thank Mathieu Lapointe and Damien Grapton for their technical assistance. This work was supported by grants from the Canadian Institutes of Health Research (MOP – 111247) and the Canadian Hemophilia Society. TM holds the Canada Research Chair (Tier 1) in Hematopoiesis and Immune Cell Differentiation.

References

1. Machlus KR, Thon JN, Italiano JE Jr. Interpreting the developmental dance of the megakaryocyte: a review of the cellular and molecular processes mediating platelet formation. Br J Haematol. 2014;165(2):227-236.
2. Nurden AT, Freson K, Seligsohn U. Inherited platelet disorders. Haemophilia. 2012;18 (Suppl 4):154-160.
3. Freson K, Wijgaerts A, van Geet C. Update on the causes of platelet disorders and functional consequences. Int J Lab Hematol. 2014;36(3):313-325.
4. Stevenson WS, Morel-Kopp MC, Chen Q, et al. GFI1B mutation causes a bleeding disorder with abnormal platelet function. J Thromb Haemost. 2013;11(11):2039-2047.
5. Monteferrario D, Bolar NA, Marneth AE, et al. A dominant-negative GFI1B mutation in the gray platelet syndrome. N Engl J Med. 2014;370(3):245-253.
6. Kitamura K, Okuno Y, Yoshida K, et al. Functional characterization of a novel GFI1B mutation causing congenital macrothrombocytopenia. J Thromb Haemost. 2016;14 (7):1462-1469.
7. Noris P, Biino G, Pecci A, et al. Platelet diameters in inherited thrombocytopenias: analysis of 376 patients with all known disorders. Blood. 2014;124(6):e4-e10.
8. Saleque S, Cameron S, Orkin SH. The zinc-finger proto-oncogene Gfi-1b is essential for development of the erythroid and megakaryocytic lineages. Genes Dev. 2002; 16(3):301-306.
9. Vassen L, Okayama T, Moroy T. Gfi1b:green fluorescent protein knock-in mice reveal a dynamic expression pattern of Gfi1b during hematopoiesis that is largely complementary to Gfi1. Blood. 2007;109(6): 2356-2364.
10. Garçon L, Lacout C, Svinartchouk F, et al. Gfi-1B plays a critical role in terminal differentiation of normal and transformed erythroid progenitor cells. Blood. 2005;105(4): 1448-1455.
11. Vassen L, Beauchemin H, Lemsaddek W, Krongold J, Trudel M, Moroy T. Growth factor independence 1b (Gfi1b) is important for the maturation of erythroid cells and the regulation of embryonic globin expression. PloS One. 2014;9(5):e96636.
12. Foudi A, Kramer DJ, Qin J, et al. Distinct, strict requirements for Gfi-1b in adult bone marrow red cell and platelet generation. J Exp Med. 2014;211(5):909-927.
13. Khandanpour C, Sharif-Askari E, Vassen L, et al. Evidence that growth factor independence 1b regulates dormancy and peripheral blood mobilization of hematopoietic stem cells. Blood. 2010;116(24):5149-5161.
14. Tiedt R, Schomber T, Hao-Shen H, Skoda RC. Pf4-Cre transgenic mice allow the generation of lineage-restricted gene knockouts for studying megakaryocyte and platelet function in vivo. Blood. 2007;109(4):1503-1506.
15. Schulze H. Culture of murine megakaryocytes and platelets from fetal liver and bone marrow. Methods Mol Biol. 2012;788: 193-203.
16. Poujol C, Ware J, Nieswandt B, Nurden AT, Nurden P. Absence of GPIbα is responsible for aberrant membrane development during megakaryocyte maturation: ultrastructural study using a transgenic model. Exp Hematol. 2002;30(4):352-360.
17. Wilkins BS, Erber WN, Bareford D, et al. Bone marrow pathology in essential thrombocythemia: interobserver reliability and utility for identifying disease subtypes. Blood. 2008;111(1):60-70.
18. Ebbe S, Boudreaux MK. Relationship of megakaryocyte ploidy with platelet number and size in cats, dogs, rabbits and mice. Comp Hematol Int. 1998;8(1):21-25.
19. Meinders M, Kulu DI, van de Werken HJ, et al. Sp1/Sp3 transcription factors regulate hallmarks of megakaryocyte maturation and platelet formation and function. Blood. 2015;125(12):1957-1967.
20. Larson MK, Watson SP. Regulation of proplatelet formation and platelet release by integrin αIIbβ3. Blood. 2006;108(5):1509-1514.

21. Humphries JD, Byron A, Humphries MJ. Integrin ligands at a glance. J Cell Sci. 2006;119(Pt 19):3901-3903.
22. Italiano JE, Jr., Lecine P, Shivdasani RA, Hartwig JH. Blood platelets are assembled principally at the ends of proplatelet processes produced by differentiated megakaryocytes. J Cell Biol. 1999;147(6): 1299-1312.
23. Avraham H, Vannier E, Cowley S, et al. Effects of the stem cell factor, c-kit ligand, on human megakaryocytic cells. Blood. 1992;79(2):365-371.
24. Ishibashi T, Kimura H, Uchida T, Kariyone S, Friese P, Burstein SA. Human interleukin 6 is a direct promoter of maturation of megakaryocytes in vitro. Proc Natl Acad Sci USA. 1989;86(15):5953-5957.
25. Clay D, Rubinstein E, Mishal Z, et al. CD9 and megakaryocyte differentiation. Blood. 2001;97(7):1982-1989.
26. Debili N, Wendling F, Cosman D, et al. The Mpl receptor is expressed in the megakaryocytic lineage from late progenitors to platelets. Blood. 1995;85(2):391-401.
27. Lim CK, Hwang WY, Aw SE, Sun L. Study of gene expression profile during cord blood-associated megakaryopoiesis. Eur J Haematol. 2008;81(3):196-208.
28. Zucker-Franklin D, Philipp CS. Platelet production in the pulmonary capillary bed: new ultrastructural evidence for an old concept. Am J Pathol. 2000;157(1):69-74.
29. Duperray A, Troesch A, Berthier R, et al. Biosynthesis and assembly of platelet GPIIb-IIIa in human megakaryocytes: evidence that assembly between pro-GPIIb and GPIIIa is a prerequisite for expression of the complex on the cell surface. Blood. 1989;74(5):1603-1611.
30. Niewiarowski S, Kornecki E, Budzynski AZ, Morinelli TA, Tuszynski GP. Fibrinogen interaction with platelet receptors. Ann N Y Acad Sci. 1983;408:536-555.
31. Huynh KC, Stoldt VR, Scharf RE. Contribution of distinct platelet integrins to binding, unfolding, and assembly of fibronectin. Biol Chem. 2013;394(11):1485-1493.
32. Jokinen J, Dadu E, Nykvist P, et al. Integrin-mediated cell adhesion to type I collagen fibrils. J Biol Chem. 2004;279(30):31956-31963.
33. Bury L, Malara A, Gresele P, Balduini A. Outside-in signalling generated by a constitutively activated integrin αIIbβ3 impairs proplatelet formation in human megakaryocytes. PloS one. 2012;7(4):e34449.
34. Baatout S, Chatelain B, Staquet P, Symann M, Chatelain C. Augmentation of the number of nucleolar organizer regions in human megakaryocyte cell lines after induction of polyploidization by a microtubule inhibitor. Eur J Clin Invest. 1998;28(2):138-144.
35. Geddis AE, Fox NE, Tkachenko E, Kaushansky K. Endomitotic megakaryocytes that form a bipolar spindle exhibit cleavage furrow ingression followed by furrow regression. Cell Cycle. 2007;6(4):455-460.
36. Thon JN, Montalvo A, Patel-Hett S, et al. Cytoskeletal mechanics of proplatelet maturation and platelet release. J Cell Biol. 2010;191(4):861-874.
37. Kunishima S, Nishimura S, Suzuki H, Imaizumi M, Saito H. TUBB1 mutation disrupting microtubule assembly impairs proplatelet formation and results in congenital macrothrombocytopenia. Eur J Haematol. 2014;92(4):276-282.
38. Chang Y, Aurade F, Larbret F, et al. Proplatelet formation is regulated by the Rho/ROCK pathway. Blood. 2007;109(10): 4229-4236.
39. Hitchcock IS, Fox NE, Prevost N, Sear K, Shattil SJ, Kaushansky K. Roles of focal adhesion kinase (FAK) in megakaryopoiesis and platelet function: studies using a megakaryocyte lineage specific FAK knockout. Blood. 2008;111(2):596-604.
40. Singh D, Upadhyay G, Sengupta A, et al. Cooperative stimulation of megakaryocytic differentiation by Gfi1b gene targets Kindlin3 and Talin1. PloS One. 2016;11 (10):e0164506.
41. Wittmann T, Bokoch GM, Waterman-Storer CM. Regulation of microtubule destabilizing activity of Op18/stathmin downstream of Rac1. J Biol Chem. 2004;279(7):6196-6203.
42. Meiri D, Marshall CB, Mokady D, et al. Mechanistic insight into GPCR-mediated activation of the microtubule-associated RhoA exchange factor GEF-H1. Nat Commun. 2014;5:4857.
43. Rudolph J, Crawford JJ, Hoeflich KP, Wang W. Inhibitors of p21-activated kinases (PAKs). J Med Chem. 2015;58(1):111-129.
44. Kosoff RE, Aslan JE, Kostyak JC, et al. Pak2 restrains endomitosis during megakaryopoiesis and alters cytoskeleton organization. Blood. 2015;125(19):2995-3005.
45. Muntean AG, Crispino JD. Differential requirements for the activation domain and FOG-interaction surface of GATA-1 in megakaryocyte gene expression and development. Blood. 2005;106(4):1223-1231.
46. Stachura DL, Chou ST, Weiss MJ. Early block to erythromegakaryocytic development conferred by loss of transcription factor GATA-1. Blood. 2006;107(1):87-97.
47. Fock EL, Yan F, Pan S, Chong BH. NF-E2-mediated enhancement of megakaryocytic differentiation and platelet production in vitro and in vivo. Exp Hematol. 2008;36(1):78-92.
48. Okada Y, Nagai R, Matsuura E, et al. Suppression of RUNX1 by siRNA in megakaryocytic UT-7/GM cells. Nucleic Acids Symp Ser (Oxf). 2006;(50):261-262.
49. Kawada H, Ito T, Pharr PN, Spyropoulos DD, Watson DK, Ogawa M. Defective megakaryopoiesis and abnormal erythroid development in Fli-1 gene-targeted mice. Int J Hematol. 2001;73(4):463-468.
50. Lecine P, Villeval JL, Vyas P, Swencki B, Xu Y, Shivdasani RA. Mice lacking transcription factor NF-E2 provide in vivo validation of the proplatelet model of thrombocytopoiesis and show a platelet production defect that is intrinsic to megakaryocytes. Blood. 1998;92(5):1608-1616.